CLAS12 Forward Time-of-Flight System Monte Carlo Simulation Details

D.S. Carman, Jefferson Laboratory

ftof-mc.tex – v1.2

April 12, 2016

Abstract

This write-up details the algorithms for the CLAS12 FTOF system for determining the ADC and TDC values for the Monte Carlo digitization routines, as well as the relevant performance and operating characteristics for this system to be modeled within the GEMC GEANT-4 Monte Carlo simulation.

1 FTOF System Overview

The Forward Time-of-Flight (FTOF) system is a major component of the CLAS12 forward detector used to measure the time-of-flight of charged particles emerging from interactions in the target. The system specifications call for an average counter timing resolution of σ_{TOF}=80 ps for θ=5° → 35° and 150 ps for $\theta > 35°$. In each of the six sectors of CLAS12, the FTOF system is comprised of three arrays of counters, referred to as panel-1a, panel-1b, and panel-2. Each panel consists of a set of rectangular scintillators with a PMT on each end. Panel-1 refers to the sets of counters located at forward angles (where two panels are necessary to meet the 80 ps average time resolution requirement) and panel-2 refers to the sets of counters at larger angles. The positioning of the FTOF system panels on the Forward Carriage of CLAS12 is shown in Fig. 1. Each of the six panel-1a arrays contains 23 counters, each of the panel-1b arrays contains 62 counters, and each of the panel-2 arrays contains 5 counters. The average path length from the target to the FTOF counters is roughly 7 m. A summary of the FTOF technical parameters is given in Table 1.

2 CLAS12 FTOF Monte Carlo

The GEANT-4 Monte Carlo suite for CLAS12 known as GEMC [1], includes realistic representations for each of the CLAS12 detector subsystems based on their nominal design parameters. To assist with this modeling, a detailed geometry specification document has been prepared for the FTOF [2] system. The simulation is designed to provide as output the same quantities that are output from the readout electronics used for the detectors, namely the ADC and TDC values associated with the measured energies and times. The digitization of these quantities must ultimately match the measured characteristics of the counters in a

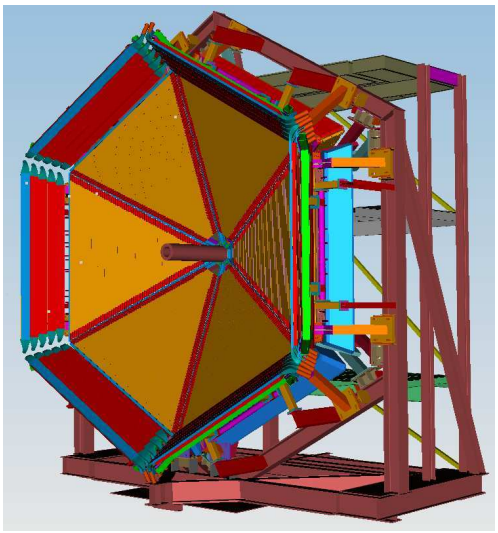

Figure 1: View of the FTOF system for CLAS12 highlighting the location of the panel-1 and panel-2 counters. The panel-1b counter arrays are shown in orange and the panel-2 counter arrays shown in red, are mounted around the perimeter of the Forward Carriage. The panel-1a counter arrays mounted just downstream of the panel-1b arrays are not visible in this picture. The Forward Carriage is roughly 10 m across.

Parameter	Design Value
Panel-1a	
Angular Coverage	$\theta = 5^\circ \rightarrow 35^\circ$, ϕ : 50% at $5^\circ \rightarrow$ 85% at 35°
Counter Dimensions	$L = 32.3$ cm $\rightarrow 376.1$ cm, $w \times h = 15$ cm $\times$ 5 cm
Scintillator Material	BC-408
PMTs	EMI 9954A, Philips XP2262
Design Resolution	90 ps $\rightarrow$ 160 ps
Panel-1b	
Angular Coverage	$\theta = 5^\circ \rightarrow 35^\circ$, ϕ : 50% at $5^\circ \rightarrow$ 85% at 35°
Counter Dimensions	$L = 17.3$ cm $\rightarrow 407.9$ cm, $w \times h = 6$ cm $\times$ 6 cm
Scintillator Material	BC-404 (#1 $\rightarrow$ #31), BC-408 (#32 $\rightarrow$ #62)
PMTs	Hamamatsu R9779
Design Resolution	60 ps $\rightarrow$ 110 ps
Panel-2	
Angular Coverage	$\theta = 35^\circ \rightarrow 45^\circ$, ϕ : 85% at $35^\circ \rightarrow$ 95% at 45°
Counter Dimensions	$L = 371.3$ cm $\rightarrow 426.1$ cm, $w \times h = 22$ cm $\times$ 5 cm
Scintillator Material	BC-408
PMTs	Photonis XP4312B, EMI 4312KB
Design Resolution	145 ps $\rightarrow$ 160 ps

Table 1: Table of design parameters for the FTOF detector system.

highly realistic manner. In this section the algorithms for determining the ADC values based on the actual deposited energy values and the TDC values based on the actual hit times are described. In addition, the FTOF parameters that allow for matching the Monte Carlo output with the actual detector parameters are detailed. The digitization is carried out in the GEMC FTOF "hit process" routine [3]. The FTOF calibration database parameters are detailed in full in Ref. [4].

The calibration database for CLAS12 (called "ccdb") includes the following parameters for the FTOF:

- Hardware status for each PMT [status]
- Attenuation length and uncertainty for each counter [attenuation]
- Effective velocity and uncertainty for each end of the counter [effective_velocity]
- Minimum ionizing peak location and uncertainty for each end of the counter [gain_balance]
- Time offset parameters (end-to-end, counter-to-counter) for each counter [timing_offset]
- Time walk constants for each end of the counter [time_walk]

In the following subsections, the algorithms for digitization of the ADC and TDC values are described in detail along with the parameters necessary to provide for a realistic Monte Carlo description of the counter responses.

2.1 ADC Digitization

The panel-1a and panel-1b detectors have been mounted on the Forward Carriage in Hall B since February 2014. At this point in time detailed gain-matching of all counters has been completed using cosmic ray muons. The gain matching was based on adjusting the high voltage settings for each PMT to position the minimum-ionizing peak for normally incident tracks in a given channel of the FADC spectrum. This procedure balances the gains of the left and right PMTs for each individual bar.

For the HV calibrations, to avoid issues with the attenuation of light for tracks that pass near the ends of the bars and to avoid issues with unbalanced photon statistics for the left and right PMTs, we combine the ADC information from the left and right PMTs to produce a geometric mean ADC spectrum for the counter through the quantity:

$$\overline{ADC} = \sqrt{(ADC_L - PED_L) \cdot (ADC_R - PED_R)}. \quad (1)$$

Given the finite dynamic range of the ADC, we have chosen to position the minimum ionizing muon peak in a particular ADC channel so that it is safely above the pedestal, but leaves sufficient range for the more highly ionizing charged tracks of our typical physics events. The position of the muon peak in the ADC spectrum is set by the PMT HV setting.

For the case of a normally incident muon passing through the extent of the counters, they deposit roughly 10 MeV as they pass through the 5-cm thick FTOF panel-1a and panel-2 counters, and roughly 12 MeV as they pass through the 6-cm thick FTOF panel-1b counters (using $dE/dx = 1.956$ MeV/cm for minimum ionizing particles in BC-404 and BC-408). Note

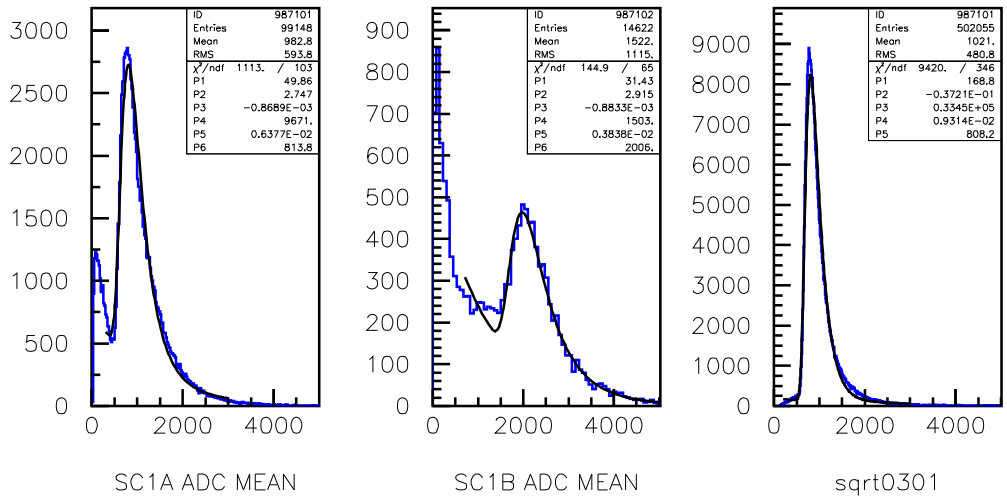

Figure 2: Average ADC spectrum for representative gain-matched counters for panel-1a (left), panel-1b (middle), and panel-2 (right). Note that the data for panel-1a and panel-1b were acquired with cosmic rays after installation of the detectors on the Forward Carriage. The data for panel-2 was acquired in the cosmic ray test stand during studies in 2013 using different cuts and a different trigger to select events.

that the ADC distribution is described by a Landau distribution sitting on an exponentially falling background.

Fig. 2 shows the average ADC spectra typical for FTOF counters in panel-1a, panel-1b, and panel-2. The panel-2 plot comes from data acquired for the counters during final assembly tests in 2013 using different cuts and a different trigger to select events compared to the panel-1a and panel-1b data that were acquired for the detector after installation on the Forward Carraige using a PCAL trigger. The panel-2 arrays are presently being installed on the Forward Carriage.

As the length of the FTOF counters in a given panel varies, adjusting the PMT HV settings to match the location of the minimum ionizing particle peak in the ADC spectrum for each counter necessarily means that the PMT gains for the longer bars are higher than for the PMT gains for the shorter bars due to attenuation length effects. Given the actual deposited energy E_{dep} in the bar, the energy measured by the left and right PMTs is given by:

$$E_L = E_{dep} \exp\left[\frac{-y_L}{\lambda_L}\right], \tag{2}$$

$$E_R = E_{dep} \exp\left[\frac{-y_R}{\lambda_R}\right], \tag{3}$$

where,

- y_L and y_R are the distances along the bar from the hit position to the left and right PMTs, respectively (see Fig. 3)
- λ_L and λ_R are the attenuation lengths for readout through the left and right ends of the counter, respectively (see Section 2.2).

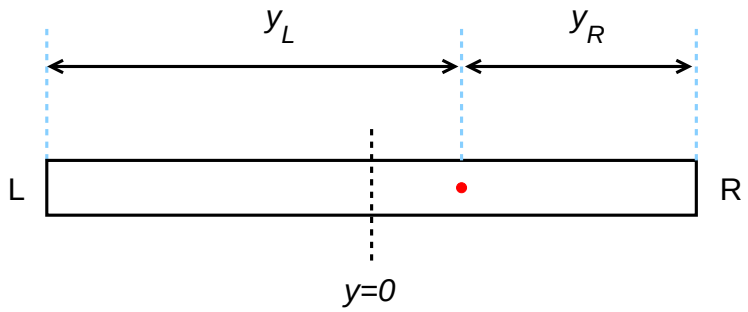

Figure 3: The track hit position along the scintillation bar is shown by the red dot and the distances along the bar from the hit point to the PMT, y_L and y_R, are shown.

The geometric mean for the deposited energy is defined as:

$$\langle E_{dep} \rangle = \sqrt{E_L E_R} = E_{dep} \left[\exp\left(\frac{-y_L}{\lambda_L}\right) \exp\left(\frac{-y_R}{\lambda_R}\right) \right]^{1/2} = \mathcal{G} E_{dep}, \tag{4}$$

where the gain factor is given by:

$$\mathcal{G} = \left[\exp\left(\frac{-y_L}{\lambda_L}\right) \exp\left(\frac{-y_R}{\lambda_R}\right) \right]^{1/2} \tag{5}$$

Accounting for this gain factor in the determination of the ADC values allows for the reproduction of the geometric mean distributions shown in Fig. 2.

The simulation determines the energy deposited in a given scintillation bar from a passing charged particle along its path. The path is defined between the hit entry point and the hit exit point. The light generated by the passing charged particle then propagates to the PMTs at either end of the bar. The conversion of the truth value of deposited energy to the recorded ADC values (ADC_L and ADC_R) must take into account that the number of generated photoelectrons at each PMT is subject to Poisson fluctuations. The digitization of the FTOF ADC values for each counter hit proceeds using the following steps:

1. Compute the energies measured by the left and right PMTs based on the deposited energy and the distances along the bar from the hit point to the PMTs as given in Eqs.(2) and (3).

2. Determine the number of photoelectrons measured by the PMTs from the computed values of E_L and E_R. Based on studies carried out with the FTOF detectors, a reasonable parameterization of the number of photoelectrons N_{pe} is given by:

$$N_{pe}^L = E_L \cdot CONV \cdot QE, \tag{6}$$
$$N_{pe}^R = E_R \cdot CONV \cdot QE, \tag{7}$$

where,

- $CONV$ = 1800 photoelectrons/MeV deposited

- $QE = 27\%$ (the quantum efficiency of the PMT).

3. Smear N_{pe} by a Poisson distribution. The resulting "smeared" number of photoelectrons based on the actual deposited energy is given by N_{pe}^{SMR}.

4. Determine the smeared values of E_L and E_R using:

$$E_L^{SMR} = \frac{N_{pe}^{L,SMR}}{CONV \cdot QE}, \tag{8}$$

$$E_R^{SMR} = \frac{N_{pe}^{R,SMR}}{CONV \cdot QE}. \tag{9}$$

5. Determine the "measured" values of the left and right ADCs using:

$$ADC_L = \frac{E_L^{SMR}}{\mathcal{K}} \cdot \frac{1}{\mathcal{G}_L} = \frac{E_L^{SMR}}{\mathcal{K}} \left[\exp\left(\frac{-y_L}{\lambda_L}\right) \exp\left(\frac{-y_R}{\lambda_R}\right)\right]^{-1/2}, \tag{10}$$

$$ADC_R = \frac{E_R^{SMR}}{\mathcal{K}} \cdot \frac{1}{\mathcal{G}_R} = \frac{E_R^{SMR}}{\mathcal{K}} \left[\exp\left(\frac{-y_L}{\lambda_L}\right) \exp\left(\frac{-y_R}{\lambda_R}\right)\right]^{-1/2}. \tag{11}$$

Here,

- The term

$$\mathcal{K} = \left[\frac{\left(\frac{dE}{dx}\right)_{MIP} \cdot t}{ADC_{MIP}}\right] \tag{12}$$

  is a conversion factor to go from ADC channel to energy.

- ADC_{MIP} = ADC value for normally incident MIPs at the center of the scintillation bar

- $\left(\frac{dE}{dx}\right)_{MIP}$ = energy loss for MIPs in the scintillation bars (1.956 MeV/cm)

- t = scintillation bar thickness (cm)

Note that in the Monte Carlo $ADC_{L,R}$ actually represents $ADC_{L,R} - PED_{L,R}$, the pedestal-subtracted ADC value from the data. Also note that the database includes separate values for λ_L and λ_R. In practice these values are the same such that $\lambda_L = \lambda_R = \lambda$.

2.2 Counter Attenuation Lengths

The attenuation length of the scintillation bars represents the distance λ into the material where the probability that the photon has been absorbed is $1/e$. For the scintillation bars, more light collected translates into better timing resolution, so it is important for the attenuation length to be as long as possible. For scintillators, it is generally hoped that the attenuation length is at least on the order of the overall length of the bars.

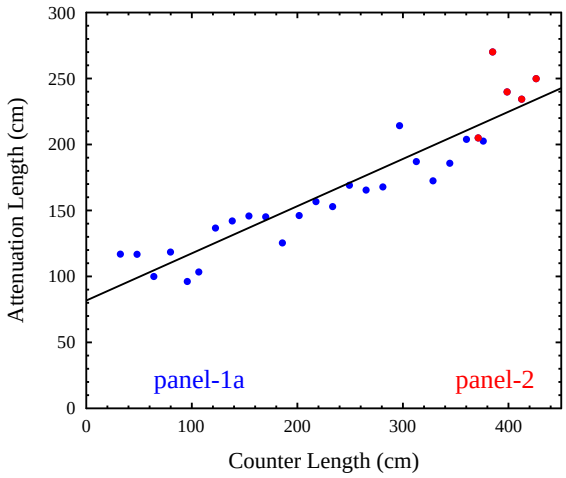

Figure 4: Average counter attenuation length for all FTOF panel-1a counters (blue points) and panel-2 counters (red points) as a function of counter length. The line is the fit from Eq.(13).

For scintillation counters there are actually two attenuation lengths that are used. The first is the attenuation length for the bulk material. For BC-404 and BC-408, this bulk attenuation length is reported by the manufacturer as 160 cm and 380 cm [5], respectively. However, the effective attenuation length for a finite geometry scintillation bar is considerably shorter to the reflections at the surfaces of the bar, which inherently depend on the specific geometry of the bar. Therefore, the true practical attenuation length of the material turns out to be about half the bulk attenuation length. The measured values from the FTOF panel-1a and panel-2 counters (see Fig.4) can be fit with a linear function to give a reasonable estimate of the attenuation length vs. counter length that is applicable for FTOF panel-1a, panel-1b, and panel-2. The fit shown in Fig. 4 is given by:

$$\lambda(\text{cm}) = 0.35771 \times L(\text{cm}) + 81.725. \tag{13}$$

3 TDC Digitization

The digitized TDC value of the hit at the left and right PMTs should account for the propagation time for light from the relevant hit point of the passing charged particle on the scintillation bar and the time-walk effects associated with the finite rise times of the signals as a function of the measured ADC values. These TDC values also must account for the time resolutions of the counters. The digitization of the FTOF TDC values for each counter hit proceeds using the following steps:

1. Compute the time walk shifts for the left and right PMTs based on the digitized values of ADC_L and ADC_R. These are given by:

$$t_L^{walk} = A_L/(ADC_L)^{B_L}, \tag{14}$$
$$t_R^{walk} = A_R/(ADC_R)^{B_R}. \tag{15}$$

During the standard FTOF system timing calibrations for physics runs, the most important corrections necessary to achieve precise timing resolutions are the time-walk corrections. Time walk is an instrumental shift in the measured hit time that arises when using leading edge discriminators. This shift in timing arises due to the finite rise time of the analog pulse. For a given event time, pulses of different amplitudes cross the discriminator threshold at slightly different times. This correction therefore depends on the ADC pulse size. Fig. 5 shows an example of the size of the correction for the panel-2 counters. Here the time residual t_r, given by the difference between the measured counter hit time and the hit time from an external source (see Ref. [6] Section 5.1), is plotted vs. the ADC value.

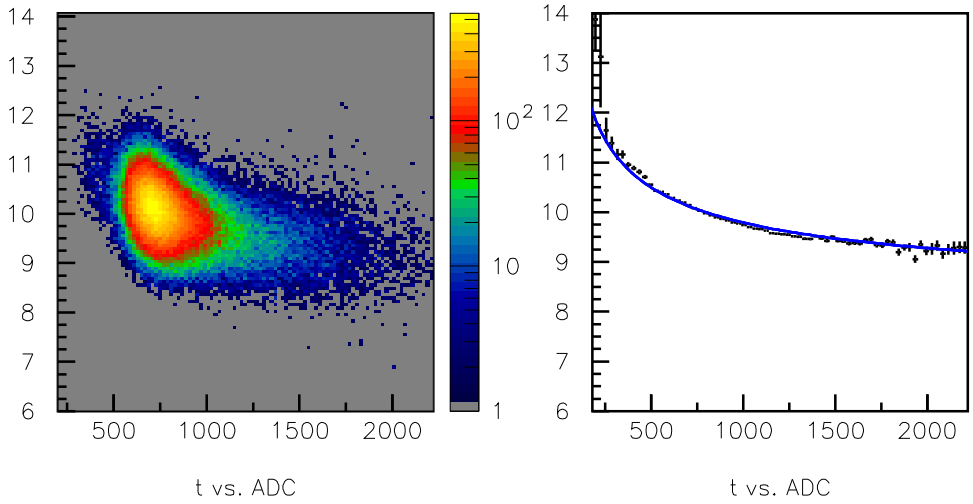

Figure 5: Plot of the measured TDC time residual (t_r in ns) for a representative panel-2 counter vs. ADC pulse height, showing the importance of time walk corrections to optimize the timing resolution. The plot on the right is the same as that on the left but shows the average t_r with statistical uncertainty vs. ADC. These data were plotted with a cut on the reconstructed coordinate along each bar to be with ± 10 cm of the middle of the counters.

2. Compute the time measured by the left and right PMTs based on the actual time of the hit t_{hit} using:

$$t_L = t_{hit} + \frac{y_L}{v_{eff}^L} + t_L^{walk}, \tag{16}$$

$$t_R = t_{hit} + \frac{y_R}{v_{eff}^R} + t_R^{walk}, \tag{17}$$

where,

- y_L and y_R are the distances along the bar from the hit position to the left and right PMTs, respectively
- v_{eff}^L and v_{eff}^R are the effective velocities of light propagation along the bar toward the left and right PMTs, respectively (see Section 3.1).

Note that the database includes separate values for v_{eff}^{L} and v_{eff}^{R}, although in practice these values are the same such that $v_{eff}^{L} = v_{eff}^{R} = v_{eff}$.

3. Smear the time values t_L and t_R based on the measured counter timing resolutions using a Gaussian distribution. The resulting "smeared" values are t_L^{SMR} and t_R^{SMR}.

   The data for the average FTOF counter timing resolutions are shown in Fig. 6. These resolutions can be parameterized using a linear fit of resolution vs. counter number as:

   - FTOF panel-1a: $\sigma_{counter}$ (ps) $= 5.45 \cdot N + 74.55$, N from $1 \rightarrow 23$
   - FTOF panel-1b: $\sigma_{counter}$ (ps) $= 0.90 \cdot N + 29.10$, N from $1 \rightarrow 62$
   - FTOF panel-2: $\sigma_{counter}$ (ps) $= 5.00 \cdot N + 145.00$, N from $1 \rightarrow 5$

   Note that the Gaussian width for the smearing of the left and right PMT times is given by:

$$\sigma_{PMT} = \sqrt{2}\sigma_{counter}. \tag{18}$$

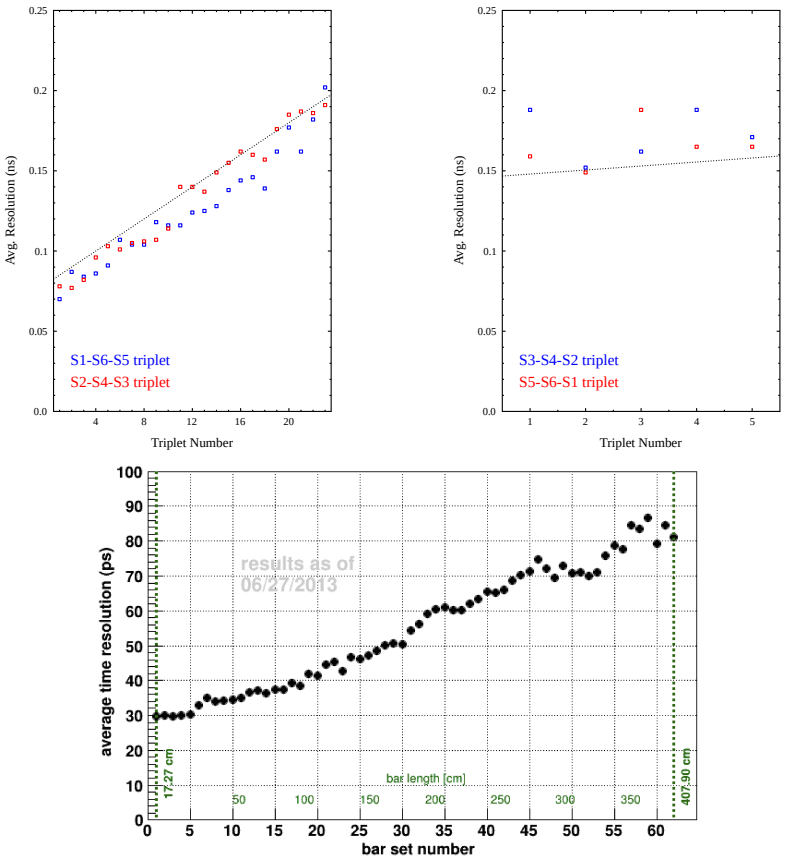

Figure 6: Average measured time resolutions for the FTOF panel-1a (upper left), panel-2 (upper right), and panel-1b (bottom) counters vs. counter number.

4. Determine the digitized values of the left and right TDCs from the smeared times using:

$$TDC_L = t_L^{SMR}/\mathcal{C}_{TDC}, \tag{19}$$
$$TDC_R = t_R^{SMR}/\mathcal{C}_{TDC}, \tag{20}$$

where $\mathcal{C}_{TDC} = 0.024$ ns/bin is the TDC channel to time conversion factor.

3.1 Effective Velocity

For initial simulation modeling, the effective velocity of all FTOF counters should be set to $v_{eff} = 16$ cm/ns. This value can be updated for the different counters after the appropriate calibration data is collected and analyzed. This value is fairly consistent for both BC-404 and BC-408 scintillation material. The data for the panel-1a and panel-2 counters from the CLAS TOF NIM paper is shown in Fig. 7 [7].

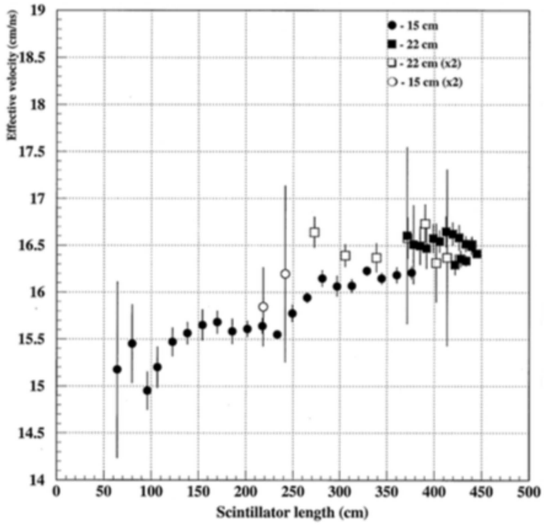

Figure 7: Average counter effective velocity (cm/ns) vs. counter length (cm) [7].

References

[1] GEMC, GEANT-4 Monte Carlo for CLAS12, http://gemc.jlab.org.

[2] D.S. Carman, FTOF Geometry Document, CLAS12-Note 2014-005, (2014).

[3] FTOF hit process routine:
https://github.com/gemc/source/blob/master/hitprocess/clas12/ftof_hitprocess.cc

[4] D.S. Carman, FTOF Calibration Constants:
http://www.jlab.org/Hall-B/ftof/notes/ftof_db.pdf.

[5] Saint-Gobain Crystals: http://www.jlab.org/Hall-B/ftof/docs/scint-spec-sheet.pdf

[6] D.S. Carman, *CLAS12 FTOF Panel-1a and Panel-2 Refurbishment and Baseline Test Results*, CLAS12-Note 2013-001, (2013).

[7] E.S. Smith *et al.*, Nucl. Inst. and Meth. A **432**, 265 (1999).